https://doi.org/10.46813/2026-164-060

STRUCTURE AND STRESS CHANGES IN LAYERED W-QC(Ti-Zr-Ni) COMPOSITIONS UNDER HYDROGEN PLASMA IRRADIATION IN THE ITER MODE

S.V. Malykhin[1], V.V. Kondratenko[1], E.N. Zubarev[1], D.V. Lytviniuk[1], I.A. Kopylets[1], S.O. Rudchenko[1,3], V.A. Makhlai[2], S.S. Herashchenko[2], I.E. Garkusha[2], S.V. Surovitsky[1], L.E. Konotopskyi[1], S.S. Borisova[1]
[1]National Technical University "Kharkiv Polytechnical Institute", Kharkiv, Ukraine;
[2]NSC "Kharkiv Institute of Physics and Technology", Institute of Plasma Physics, Kharkiv, Ukraine;
[3]Technical University of Denmark, Department of Civil and Mechanical Engineering, 2800 Kongens Lyngby, Denmark
E-mail: Serhii.Malykhin@khpi.edu.ua

Using X-ray diffraction and scanning electron microscopy, changes in the structural and stress state in layered W/QC/steel, QC/W/steel, and W/steel magnetron-deposited composites, as well as in bulk tungsten samples, irradiated with hydrogen plasma at a thermal load of up to 0.6 MJ·m^{-2}, were studied. According to the results of irradiation of bulk samples and magnetron coatings, annealed and unannealed, the changes in macrostresses, structure and substructure caused by plasma irradiation are determined by the structure in the initial state: namely, the type, density and distribution of dislocations and point defect complexes. The initial residual internal compressive stresses decrease with an increase in the number of plasma irradiation pulses, regardless of their initial level and the magnitude of the thermal effect, with a subsequent transition to tensile stresses. The scale and rate of the stress reduction vary for different compositions. Taking into account the studied features of layered systems based on W and Ti-Zr-Ni quasicrystals under conditions of radiation-thermal loads of varying intensity and dose, these compositions are proposed to be used to increase the radiation resistance of materials in nuclear and thermonuclear energy.

PACS: 52.40.HF

INTRODUCTION

As a result of solving the materials science problem aimed at increasing the service life of the diverter plates and the first wall of the ITER thermonuclear reactor, new physical and chemical patterns of radiation-induced phenomena in materials during interaction with plasma will be obtained, and stable composite systems and structures will be developed on their basis [1, 2]. By now, a significant amount of knowledge has been accumulated regarding the behavior of tungsten diverter plates during current disruptions, vertical displacement events, and boundary localized modes that will accompany the operation of next-generation fusion facilities such as ITER and DEMO [3–7]. For them, tungsten was chosen as the main material for the blanker space due to its high thermal conductivity, thermal strength, melting point and low sputtering coefficient [7, 8]. However, the gradual accumulation of internal macrostresses and the development of surface cracks lead to significant macroscopic erosion, and the accumulation of deuterium and tritium isotopes, as well as helium atoms, can result in embrittlement of tungsten [9, 10]. Tungsten coatings on various substrates can be a less expensive alternative to bulk tungsten for first wall protection. It is known that ion-plasma and, in particular, magnetron-deposited tungsten coatings of micron thickness have a very high (up to 2...3 GPa) level of internal compressive stresses [11, 12]. It can be assumed that such stresses will prevent the initiation and propagation of cracks, which will extend the service life of the material under cyclic plasma loads. In addition, it has also been proposed to use a Ti-Zr-Ni quasicrystal (QC) layer to protect tungsten, as well as steel, from hydrogen embrittlement. It is known that Ti-Zr-Ni QCs are capable of reversibly absorbing hydrogen in quantities up to 2H/at in the form of a solid solution without the formation of hydrides [13].

In this work, the objective was to experimentally investigate the behavior of various layered compositions of tungsten and Ti-Zr-Ni quasicrystal under radiation-thermal conditions close to the operation of the ITER thermonuclear reactor. It is assumed that the layered W/QC and QC/W systems will be able to demonstrate themselves as modern nanostructured SMART systems, in which each layer performs its own function.

1. SAMPLES AND INVESTIGATION TECHNIQUE

To accomplish the task set in the work, layered coatings of three compositions were produced on substrates made of sheet steel Kh18N9T steel (Table), namely: W(2 μm)/steel (composition 1); $Ti_{41}Zr_{41}Ni_{18}$ QC (5.4 μm)/W(2 μm)/steel (composition 2) and W(2 μm)/ $Ti_{41}Zr_{41}Ni_{18}$ QC (5.4 μm)/steel (composition 3). The layered coatings were formed by direct-flow magnetron sputtering of a target alloy with the composition $Ti_{41}Zr_{38.3}Ni_{20.7}$ (at.%) and a tungsten target (99.8%) in an Ar environment. The samples were made in duplicate. One sample from each composition was annealed. Vacuum annealing was carried out for 60 h at T=753 K. This annealing regime ensured the formation of a quasicrystalline icosahedral phase from the initially amorphous one.

The coatings were irradiated with a hydrogen plasma flow at the QSPA X-50 quasi-stationary plasma accelerator (NSC KIPT). The main parameters of the QSPA plasma flux were as follows: ion impact energy up to 0.4 keV, maximum plasma pressure of 0.32 MPa and flux diameter of about 18 cm. The pulse duration was 0.25 ms. The number of pulses ranged from 5 to 15. The thermal load was 0.6 MJ/m^2, which determined the heating value of the tungsten surface to 2587 K (0.7T_m) [14].

The morphology of cross-sections of the samples was studied using scanning microscopy with a Zeiss Sigma 300 SEM. The structural characteristics and residual internal stresses were determined using the XRD method. Diffraction measurements were carried out using filtered Cu-K_α radiation. The thickness of the tungsten layer in the coatings was 2 μm, which corresponds to approximately two half-absorption layers for λ-Cu. Thus, the information obtained was integral over the entire thickness of the layer. The New_Profile 3.5 software package was used to process diffraction patterns. Information on the structural state was obtained by determining the position (2ϑ), FWHM (full width at half maximum of the diffraction maximum) (B) and intensity of the diffraction maxima. Residual macrostresses (σ) and the lattice period in the unstressed state (a_0) were determined from the a-sin$^2\psi$ graphs constructed based on the (400) or (321) lines located in the angle range between 151 and 127…131 deg for precision measurements. The nature of the intensity distribution in the diffraction maximum profile was also analyzed and the symmetry (asymmetry) of the profile was determined. To quantitatively characterize the asymmetry of the diffraction maximum, the asymmetry parameter (δB) is introduced as the ratio of the difference between the left (B_l) part (in relation to the top) and the right part (B_r) of the FWHM to the entire width: $\delta B = \frac{B_l - B_r}{B_l + B_r}$.

2. RESULTS

2.1. CHARACTERIZATION OF THE INITIAL STATE

2.1.1. The initial state of the quasi-crystalline layer of composition No. 2

Fig. 1,a shows a diffraction pattern from a sample of the composition No. 2 coating in its initial state. It can be seen that after deposition the coating was amorphous. According to the results, after annealing for 60 h at a temperature of 753 K, the amorphous phase transforms into a quasicrystalline icosahedral phase (QC) (Fig. 1,b). In addition, traces of the 2/1 phase of the crystalline approximant are present. Reflections from the QC phase in the figure are marked with double J. Cahn indices [15]. The quasi-crystallinity parameter a_q of the QC phase before plasma irradiation is about 0.5208 nm, and the FWHM of the (18.29) reflection is ≈9.6 μrad.

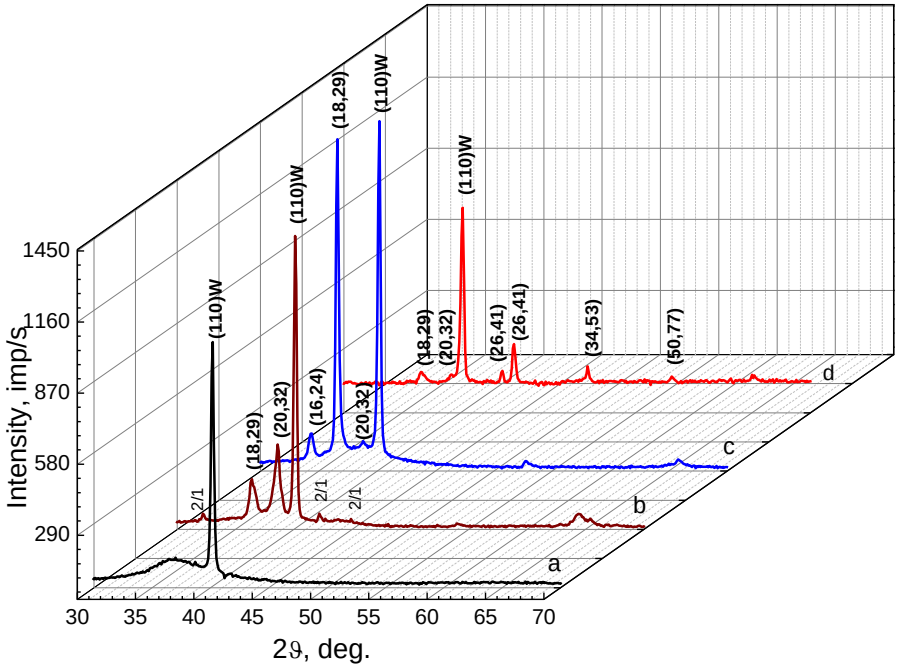


Fig. 1. Diffraction patterns obtained in Cu-K_α from sample No. 2 in the initial state (a); after long-term vacuum annealing (b); after irradiation with hydrogen plasma with a thermal load of 0.6 MJ·m^{-2} with 5 (c), and 10 (d) pulses

2.1.2. Features of the structural state of the tungsten layer of the compositions

The SEM image of the cross-section of composition No. 1 is shown in Table. As can be seen from the image (a), the tungsten layer has a fibrous columnar microstructure, characteristic of magnetron-deposited coatings of refractory elements at relatively low values of working gas pressure [12, 13]. According to XRD data, the coating is textured. It formed a preferential orientation of axial-type grains with the axis of symmetry [110] along the normal to the surface. The width of the rocking curve for the (110) reflection is about 15 deg, which indicates low texture perfection of the tungsten layer.

According to X-ray tensometry studies taking into account the texture of the samples, residual compressive

stresses act in the tungsten layers of the coatings. Evidence of the latter fact is the sign of the slope of the a-$sin^2\psi$ graphs presented in Fig. 2,a and b, for coatings in the initial state and after long-term annealing, respectively (the numbers on the dependencies correspond to the numbers of the compositions). According to calculations, the stress value for all the coatings studied ranges from -0.6 to -1.4 GPa. It should be noted that the sign and magnitude of stresses in the studied tungsten layers are in good agreement with the data of works [12, 13] indicating that the stresses exceed 1 GPa and must be compressive. The stresses arise from the accumulation of structural defects that form in the growing coating due to the simultaneous implantation of native atoms and, possibly, atoms of the working gas. The qualitative change in the appearance of a-$sin^2\psi$ graphs under radiation exposure is discussed in detail in [16].

The analysis showed a connection between changes in the a-$sin^2\psi$ graphs and the accumulation of point defects and dislocation loops in the bulk of thin films, as well as their transformation into half-planes. The effect of accumulation of structural defects is clearly observed in the given a-$sin^2\psi$ graphs (see Fig. 2). From Fig. 2,a it is evident that the value of the lattice period in the isotropic section (vertical line) significantly exceeds the tabular value for pure bulk tungsten, a_{tb}=0.31652 nm (marked in the figure by the horizontal line).

Based on the results of [16], it can be stated that the tungsten layer of all coatings contains complexes of excess interstitial atoms. This is also evidenced by the fact of asymmetry of diffraction profiles. The asymmetry is associated with the presence of an additional diffuse maximum near the diffraction maximum. In the presence of interstitial complexes, the diffuse maximum is located to the right of the main maximum, and the asymmetry parameter will be negative. This is observed for all coatings in the initial state.

In addition, one should pay attention to the difference in the slope of the graphs in Fig. 2,a. The difference is due to the spread of the values of the lattice periods along the normal to the surface – a_{perp}, and in the plane of the coating – a_{parl}, when moving from one sample to the next. The difference may indicate that immediately after deposition in the W layer, in addition to interstitial complexes, interstitial dislocation loops located at an angle to the surface arise [16].

Long-term annealing of the compositions at a temperature of only $0.2T_m$ led to a qualitative change in the appearance of the a-$sin^2\psi$ graphs (see Fig. 2,b). This temperature effect is just sufficient for the migration and redistribution of interstitial atom complexes [17]. It is clear that the a_{perp} for the three compositions converged to approximately one point, and all the differences lie in the value of a_{parl}.

The observed effect can be interpreted as a result of the reorientation of interstitial loops predominantly perpendicular to the surface. This effect in coatings of all compositions is accompanied by a decrease in the FWHM of the diffraction maximum (321) W by an average of 15%, and indicates an integral decrease in the concentration of dislocation-type defects, presumably due to the sorption of some interstitial atoms.

2.2. CHANGES IN THE STRUCTURAL-STRESS STATE OF COATINGS AS A RESULT OF PLASMA IRRADIATION

According to the diffraction patterns presented in Fig. 1,c and d, the quasi-crystalline phase is preserved as a result of irradiation with hydrogen plasma up to 10 pulses.

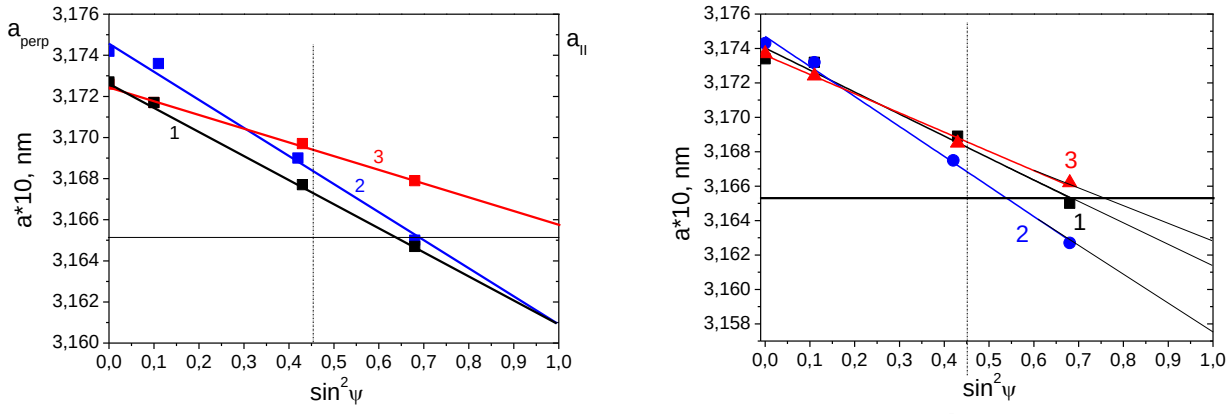
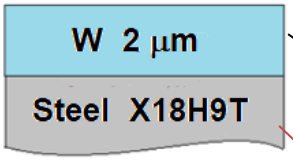
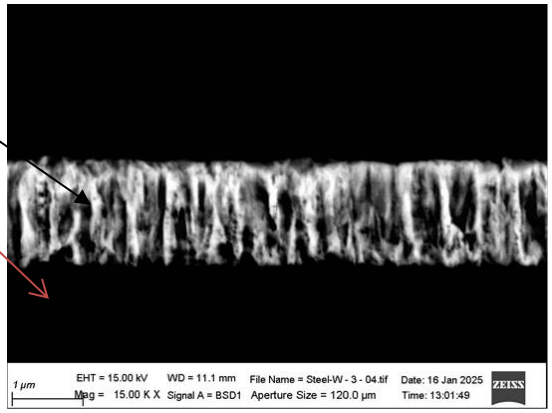
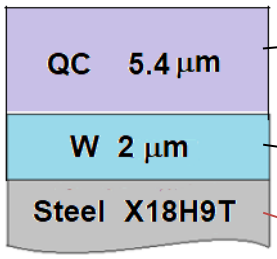
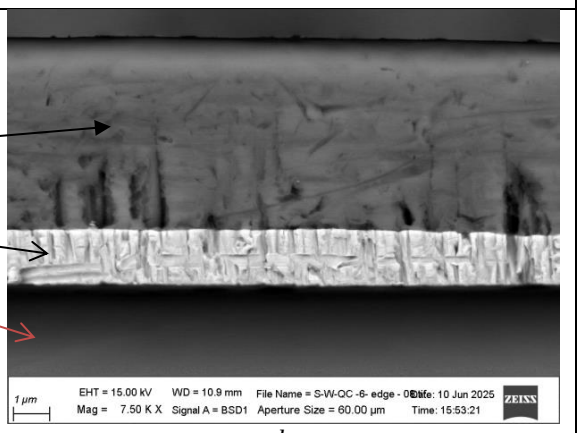
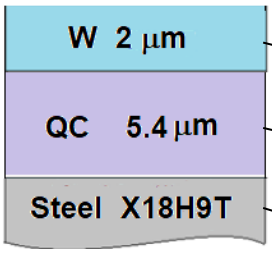
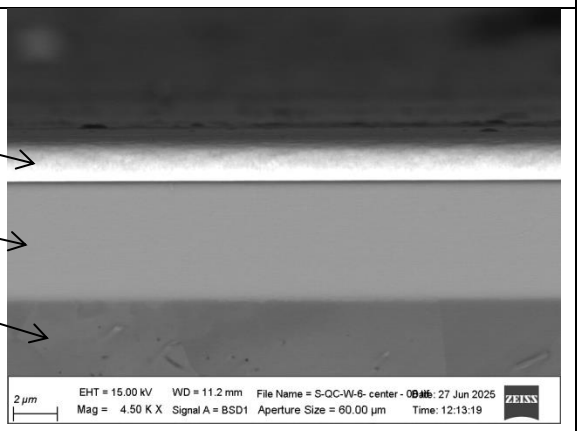


Fig. 2. a-$sin^2\psi$ – graphs for the tungsten layer of the studied compositions in the initial state (a) and after annealing (b)

After 5 pulses of irradiation, reflections from the crystalline approximant phase disappear. After each irradiation, the QC phase undergoes recrystallization. This is manifested in a change in the number of reflections from this phase and a change (redistribution) of intensity between the reflections.

According to calculations performed in [14], at a thermal load of 0.6 MJ·m^{-2}, the surface of the sample is short-term heated to a temperature of 2580 K (0.7 T_m). Consequently, the quasicrystalline layer is subjected to melting and subsequent high-speed quenching. In this case, the QC phase on the surface is preserved. The diffraction peaks from QC shift towards larger diffraction peaks, and the quasi-crystallinity parameter a_q decreases. The latter fact is somewhat strange, since when hydrogen dissolves in the QC structure, the quasi-crystallinity parameter should increase. It is assumed that the decrease in the parameter a_q, specifically by ≈ 0.3% along the normal to the surface, occurs as a result of the formation of tensile stresses.

Samples under study, diagrams and designations of film coating compositions, as well as SEM images of cross-sections of coatings in the initial state in the light of reflected electrons

Composition No. 1		 *a*
Composition No. 2		 *b*
Composition No. 3		 *c*

When an unannealed sample is irradiated with 5 pulses, a phase transformation occurs, the halo from the amorphous phase disappears, and reflections from the quasi-crystalline phase with a quasi-crystallinity parameter equal to 0.5155 nm are formed on the diffraction pattern. For comparison, in the sample after long-term annealing, the parameter a_q was 0.5190 nm. This fact indicates that the QC phase obtained by annealing has a more perfect structure than that obtained by irradiation. As a result of irradiation, the approximant phase is not formed and its reflections are not observed in the diffraction pattern. With an increase in the number of pulses to 10, there is a slight decrease in the parameter a_q to 0.5140 nm, most likely associated with the formation of compressive stresses in the QC layer.

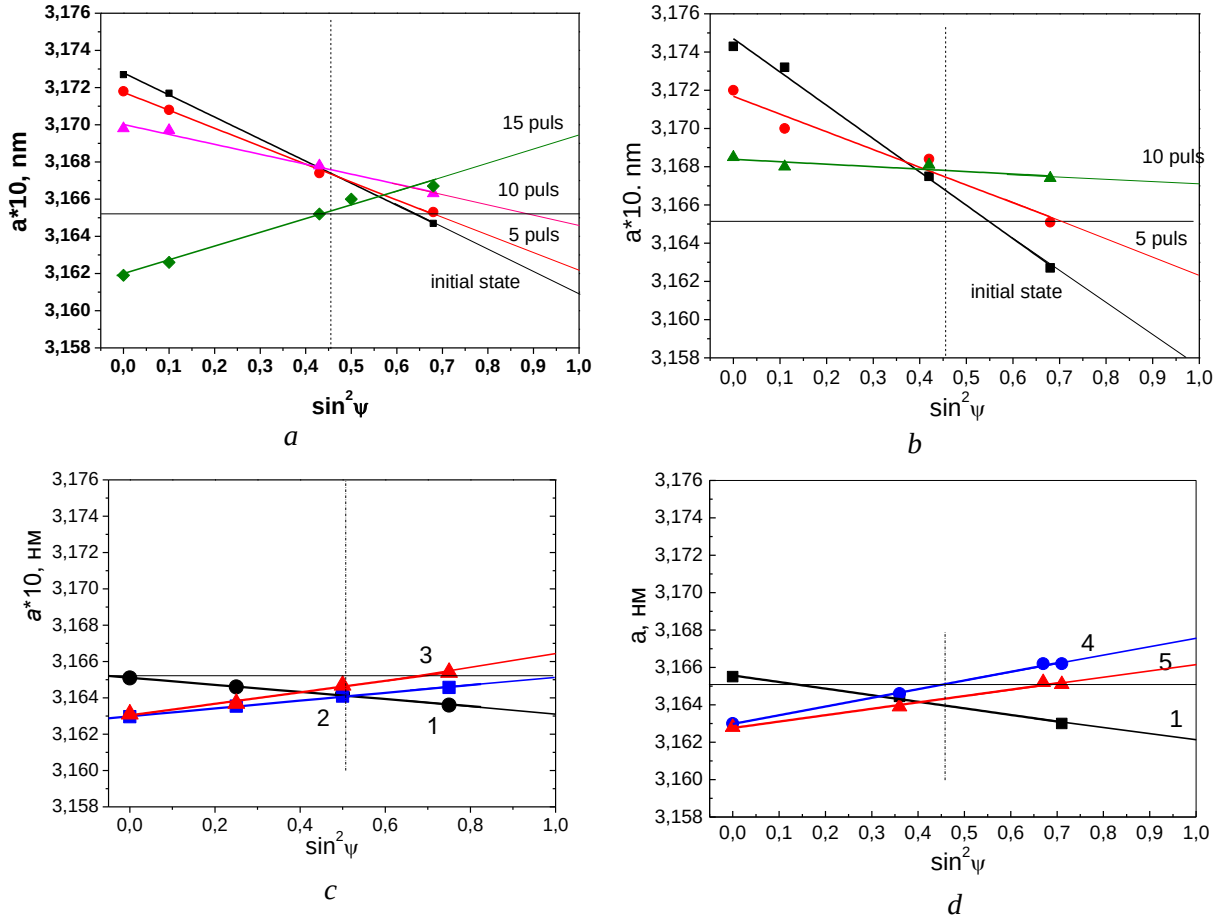


Fig. 3. Examples of a-sin²ψ-graphs for tungsten coating of composition No. 1 in the initial state (a) and annealed (b), as well as for bulk tungsten, where (1) is the initial state; after irradiation with hydrogen plasma with a thermal load of 0.3 MJ ·m^{-2} (c): (2) – 2 pulses, (3) – 50 pulses; after irradiation with 0.45 MJ ·m^{-2}(d): (4) – 10 pulses and (5)– 100 pulses [6]

Under the influence of plasma irradiation in the tungsten layers of all compositions, with an increase in the number of pulses, a change in the stress state occurs. The gradual decrease in the magnitude of residual compressive stresses is indicated by the change in the slope of the *a-sin²ψ* graphs. As an example, Fig. 3 shows the corresponding graphs for the tungsten layer of the composition No.1 for the initial state (a) and annealed (b) at different quantities of irradiation pulses. The graphs for the other two compositions have a similar appearance. According to the figures shown, the initial compressive stresses gradually decrease as a result of irradiation, and in the layer of unannealed tungsten (see Fig. 3,a), after 15 irradiation pulses, the stresses become tensile.

The generalized dependences of the magnitude of residual internal stresses in the tungsten layer of all studied compositions in the initial state (a) and after annealing (b) change with an increase in the number of plasma irradiation pulses, as shown in Fig. 4. It can be seen from the figures that with the accumulation of the number of irradiation pulses, annealing of the initial compressive stresses occurs, and eventually the stresses transform into tensile stresses.

According to Fig. 4,c and d, annealing of the initial stresses is accompanied by a decrease in the lattice period in the unstressed section. The period a_0 for an unstressed section $sin^2\psi_0 = \frac{2\nu}{1+\nu}$ (as if minus the stress) with an increase in the number of irradiation pulses tends to reach, and in some cases reaches, the tabulated value for pure tungsten. The only exception is the W coating No. 2, which has undergone preliminary long-term annealing. It is characterized by a small increase in the lattice period, which only slightly exceeds the measurement error.

For comparison, Fig. 3,c and d show *a-sin²ψ* graphs for bulk tungsten samples in the initial state and those irradiated with hydrogen plasma with a thermal load of 0.3 and 0.45 MJ·m^{-2} [6]. It can be seen that in the initial state after mechanical polishing, compressive stresses also act in the surface layer. However, their value was from 200 to 400 MPa, which is significantly less than in coatings.

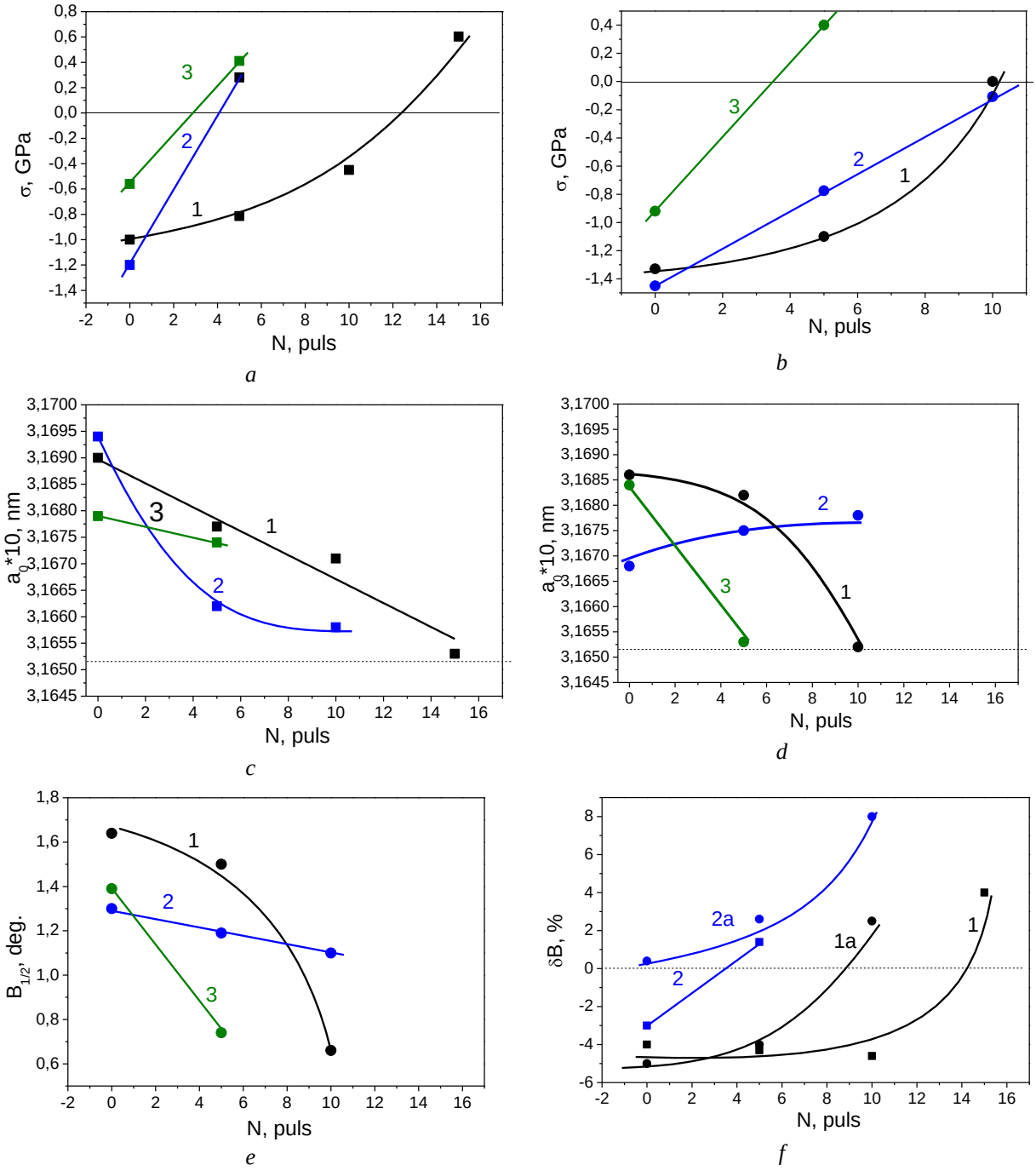


Fig. 4. Change of the magnitude of residual stresses in the tungsten layer of compositions No. 1 (1), No. 2 (2), No. 3 (3) in the initial state (a) and after annealing (b); the lattice parameter in the unstressed state (c) and (d); the FWHM width of the reflection (321) in the initial state (e); the asymmetry of the reflection (321) for the compositions No. 1 and 2 in the initial and annealed (a) states (f)

Since the graphs are plotted on the same scale, this can be seen clearly. As a result of irradiation, these stresses are quickly annealed and transform into tensile stresses. With an increase in the irradiation load from 0.1 to 0.8 MJ·m^{-2}, tensile stresses increase according to a parabolic law from 100 to 450 MPa [6].

The width of the (400) reflection decreases by approximately 27% with an increase in the number of pulses to 50. A characteristic feature of bulk samples obtained by hot pressing and subsequent deformation is the presence of vacancy-type complexes in the volume. It can be seen from the Fig. 4,c,d that their content significantly reduces the value of the lattice period in the unstrained section. Irradiation of samples with plasma anneals these complexes, resulting in the lattice period a_0 increasing up to the tabulated value.

DISCUSSION

High compressive stresses in magnetron tungsten coatings, according to [11, 12], have a structural nature. In this work, textured [110] W layers with a thickness of 2 μm, obtained by magnetron sputtering, in the initial state are characterized by compressive stresses of σ = -0.6…-1.4 GPa and have an increased value of the crystal lattice parameter in the unstrained section a_0 = 0.31680…0.31695 nm compared to the tabulated

value, a = 0.31652 nm. Compressive stresses and an increased value of the crystal lattice parameter are caused by the formation of small flat interstitial complexes in the coating during its production under the action of bombardment of the growing surface by sputtered W atoms with increased energy and Ar atoms reflected from the tungsten target.

In a coating fixed to a substrate, the lattice period in the coating plane a_{parl} cannot change, but the lattice period in the unstrained section a_0 and the lattice period along the normal to the surface a_{perp} increase. As a result, the slope of the a-$sin^2\psi$ graphs becomes negative, which indicates significant compressive stresses in the initial state. In bulk tungsten samples, relatively small compressive stresses in the initial state, which have been repeatedly observed previously [6, 14, 20, 21], are caused by polishing the surface of the samples before plasma irradiation.

The nature of the tensile stresses that arise during irradiation is in the non-uniform thermal effect across the thickness, when the surface heats up significantly, while the layers lying deep inside remain cold. Under the influence of temporary stresses, the surface layer with a thickness of about 1 μm is irreversibly plastically deformed, while the internal layers only elastically expand thermally. After removal of the irradiation effect and cooling, tensile stresses should form [18, 19]. The non-uniform thermal effect across the cross-section, increasing with increasing irradiation dose, ultimately leads to annealing of the initial compressive structural stresses.

The decrease in the initially overestimated period a_0 and residual stresses during plasma irradiation, compared to the tabular data, can be explained by the occurrence of two processes. The first is the sorption of excess interstitial atoms and small complexes by dislocations and dislocation loops. At the same time, the latter can move, open and form extra planes. The second process is associated with the fact that a surface heated to 0.7 T_m is capable of generating a flow of vacancies into the coating volume. Vacancies can interact with complexes of interstitial atoms with subsequent annihilation and with dislocations. Both processes affect the FWHM width of the reflections and their asymmetry, which is observed in Fig. 4,e and f. As can be seen from Fig. 4,e, the width of the reflection (321) in compositions No.1 and 3, in which the tungsten layer is external, decreases more intensively. The FWHM width decreases from 30 to 20 mrad, which means a decrease in the concentration of dislocations randomly distributed in the grain volume.

Some features appear on the dose dependences of the tungsten crystal lattice period and the FWHM width and the reflection asymmetry (321) in composition No. 2 (QC/W/steel). This is clearly seen in Fig. 4,d,e,f. It is evident that the lattice period a_0 does not decrease. The negative asymmetry caused by interstitial atom complexes is completely eliminated after long-term annealing. These effects can be explained by the fact that at an annealing temperature of 0.2 T_m, according to [17, 22], interstitial atoms and their small complexes are mobile. Consequently, they are capable of settling on dislocation loops and dislocations, which causes their non-conservative movement. As a result, the FWHM of the (321) reflection decreased by 27% after annealing.

When this composition is plasma irradiated, the FWHM decreases more slowly than in tungsten coatings of compositions No.1 and 3. We assume that this is due to the fact that the flow of vacancies from a surface heated to 0.7 T_m through the quasicrystal layer is significantly suppressed. In addition, as can be seen from Fig. 4,f, the remaining part of the vacancies contributes to the formation of complexes. Taking into account that the dependence associated with the removal of residual internal stresses (see Fig. 4,b) under the QC is linear, while without the QC layer it is close to parabolic, it can be argued that the quasi-crystalline layer has fulfilled its protective function to some extent.

It also cannot be ruled out that at such high temperatures the layer of the quasicrystalline phase is in a liquid state and interaction of its components (Ti and Zr) with the tungsten layer becomes possible. Such dissolution should lead to an increase in the lattice parameter of tungsten, since the atomic radii of Ti and Zr are larger than the atomic radius of W. This increase can compensate for its decrease due to the dissolution of interstitial clusters.

CONCLUSIONS

1. An experimental study was carried out on the effect of hydrogen plasma irradiation with a thermal load of 0.6 MJ/m^2 and a dose of up to 15 pulses on the structural-phase and stress state of tungsten layers and $Ti_{41}Zr_{41}Ni_{18}$ quasicrystal of three compositions on a substrate of Kh18N9T steel.

2. The obtained results demonstrate using specific examples that the irradiation-induced changes in internal macrostresses, structure and substructure parameters of the irradiated material depend on the type, density and distribution of dislocation complexes and point defects of the initial state of the structure, and on the direction and diffusion parameters of point defects generated by the heated surface.

3. It has been established that the icosahedral quasicrystalline phase is stable under the selected experimental temperature-plasma loads, and the phase of the crystalline 2/1 approximant undergoes a transformation into the quasicrystalline phase.

4. The established differences in the behavior of the characteristics of the structure and the stress state in the tungsten layer in the QC/W/steel composition in comparison with the W/steel and W/QC/steel compositions allow us to assert that, under conditions of high radiation-thermal load of 0.6 MJ/m^2, this composition is of interest for further research.

5. The results obtained in the work, namely the establishment of the mechanisms of structural and phase changes by studying diffusion, mixing between layers, phase transformations, the development of internal macrostresses, changes in the characteristics of the structure and microstructure, can be used to create radiation-resistant materials.

ACKNOWLEDGEMENT

The work was carried out with financial support of the National Research Fundation of Ukraine (Grant

2025.07/0302 “Scientific rationale, development, and testing of functional protective coatings for reactor components under radiation plasma conditions”).

REFERENCES

1. G. Pintsuk et al. Materials for in-vessel components // *Fusion Engineering and Design*. 2022, v. 174, p. 112994.

2. J.H. You et al. Limiters for DEMO wall protection: Initial design concepts & technology options // *Fusion Engineering and Design*. 2022, v. 174, p. 112988.

3. F. Maviglia et al. Impact of plasma-wall interaction and exhaust on the EU-DEMO design // *Nuclear Materials and Energy.* 2021, v. 26, p. 100897.

4. R. Neu et al. Investigations on cold spray tungsten/tantalum coatings for plasma facing applications // *Nuclear Materials and Energy*. 2023, v. 34, p. 101343M.

5. V.A. Makhlaj et al. Plasma exposure of different tungsten grades with plasma accelerators under ITER relevant conditions // *Physica Scripta*. 2014, v. T161, p. 014040.

6. V.A. Makhlai et al. Damaging of tungsten and tungsten – tantalum alloy exposed in ITER ELM-like// *Nuclear Materials and Energy*. 2016, v. 9, p. 116-122.

7. Philipps V Tungsten as material for plasma-facing components in fusion devices // *J. Nucl. Mater.* 2011, 415, 1, Suppl 1, p. S2-S9.

8. Piazza, G. Matthews, G.F. Pamela, J. Altmann, et al. R&D on tungsten plasma facing components for the JET ITER-like wall project // *Journal of Nuclear Materials.* 2007, v. 367-370. p. 1443; doi:10.1016/j.jnucmat.2007.04.039

9. I.E. Garkusha et al. Structure evolution of tungsten coatings exposed to plasma flows under iter ELM relevant conditions // *Technical Physics*. 2014, v. 59, N 11, p. 1620-1625.

10. I.S. Landman et al. Material Surface Damage under High Pulse Loads Typical for ELM bursts and disrupttions in ITER // *Physica Scripta.* 2004, v. T111, p. 206.

11. J.A. Thornton, D.W. Hoffman. Stress-related effects in thin films // *Thin Solid Films*. 1980, v. 171, N 1, p. 5-31.

12. E.N. Zubarev, A.V. Zhurba, et al. The structure, diffusion and phase formation in Mo/Si multilayers with stressed Mo layers // *Thin Solid Films.* 2007, v. 515, p. 7011-7019.

13. A.M. Viano et al. Hydrogen absorption and storage in quasicrystalline and related Ti-Zr-Ni alloys // *Philos. Mag. A.* 1998, v. 78, p. 131-142; https://doi.org/10.1080/014186198253714

14. V.A. Makhlaj, I.E. Garkusha, N.N. Aksenov, et al. Tungsten damage and melt losses under plasma accelerator exposure with ITER ELM relevant conditions // *Physica Scripta*. 2014, v. 159, p. 014024; DOI: 10.1088/0031-8949/2014/T159/014024

15. J. Cahn, D. Shechtman, D. Grafias. Indexing of icosahedral quasiperiodic crystals // *J. Mat. Res.* 1986, v. 1, N 1, p. 30-54.

16. S. Malykhin, I. Mikhailov. S. Borisova X-ray methods for analyses of condensed films // *Transactions on Physics & Math in Engineering Science*. 2025, Series A: Materials & Technology, v. 2, 84 p.

17. A.M. Shalaev. *Structure and properties of metals and alloys: Reference: Properties of irradiated metals and alloys.* Kiev: “Naukova Dumka”, 1985, 308 p.

18. L.I. Gladkikh, S.V. Malykhin, A.T. Pugachev. *Diffraction methods for analyzing internal stresses. Theory and experiment*: Textbook. Kharkiv: NTU “KhPI”, 2006, 304 p.

19. I.C. Noyan and J.B. Cohen. *Residual Stress.* New York: Springer, 1987.

20. V.A. Makhlaj et al. Residual stresses in tungsten under exposures with ITER ELM-like plasma loads // *Phys. Scr*. 2009, v. 138, p. 014060 (5 p.); doi:10.1088/0031-8949/2009/T138/014060

21. I Garkusha, V Makhlaj, et al. Materials surface damage and modification under high power plasma exposures // *IOP Conf. Series: Journal of Physics: Conf. Series.* 2018. v. 959, p. 012004; doi :10.1088/1742-6596/959/1/012004

22. F.F. Komarov. *Ion implantation in metals*. M.: “Metallurgy”, 1990, p. 216.

Article received 09.06.2926

ЗМІНЕННЯ СТРУКТУРИ ТА НАПРУЖЕНЬ У ШАРУВАТИХ КОМПОЗИЦІЯХ W-QC(Ti-Zr-Ni) ПІД ДІЄЮ ОПРОМІНЕННЯ ВОДНЕВОЮ ПЛАЗМОЮ В РЕЖИМІ ІТЕР

С.В. Малихін, В.В. Кондратенко, Є.М. Зубарєв, Д.В. Литвінюк, І.А. Копилець, С.О. Рудченко, В.О. Махлай, С.С. Геращенко, І.Є. Гаркуша, С.В. Суровицький, Л.Є. Конотопський, С.С. Борисова

Методами рентгенівської дифрактометрії та скануючої електронної мікроскопії вивчені змінення структурного та напруженого стану в шаруватих композиціях W/QC/сталь, QC/W/сталь та W/сталь, отриманих магнетронним розпиленням, та в зразках масивного вольфраму при опроміненні водневою плазмою до 0,6 МДж·м$^{-2}$. Згідно з результатами опромінення масивних зразків та магнетронних покриттів, що пройшли відпал і без відпалу, встановлено, що стимульовані плазмовим опроміненням зміни внутрішніх макронапружень, характеристик структури та субстуктури визначаються структурою у вихідному стані. А саме типом, густиною та розподілом комплексів дислокацій та точкових дефектів. Вихідні залишкові внутрішні напруження стискування знижуються зі збільшенням кількості імпульсів плазмового опромінення незалежно від їх вихідного рівня та від величини теплового впливу з подальшим переходом у напруження розтягу. Масштаб та швидкість зниження різні для різних композицій. Вказані композиції з урахуванням вивчених особливостей поведінки шаруватих систем на основі W та Ti-Zr-Ni квазікристалу в умовах радіаційно-термічного навантаження різної інтенсивності та дози пропонується використовувати для підвищення радіаційної стійкості матеріалів у ядерній та термоядерній енергетиці.